

Nonlocal Josephson diode effect in minimal Kitaev chains

Jorge Cayao¹ and Masatoshi Sato²

¹Department of Physics and Astronomy, Uppsala University, Box 516, S-751 20 Uppsala, Sweden

²Yukawa Institute for Theoretical Physics, Kyoto University, Kyoto 606-8502, Japan

(Dated: December 2, 2025)

We study the emergence of the nonlocal Josephson effect in a system composed of three laterally coupled minimal Kitaev chains and exploit it to realize the nonlocal Josephson diode effect. We find that an imbalance between crossed Andreev reflections and electron cotunneling in the middle Kitaev chain gives rise to an asymmetric 2π -periodic phase-dependent Andreev spectrum, controlled by the superconducting phases across the left and right junctions. We then show that the asymmetric Andreev spectrum, formed by hybridized Andreev bound states at the left and right junctions, enables a supercurrent across one junction via the phase difference at the other junction, thereby signaling the nonlocal Josephson effect. Notably, these nonlocal Josephson supercurrents exhibit distinct positive and negative critical currents, demonstrating the realization of the nonlocal Josephson diode effect with highly tunable polarity and efficiencies exceeding 50%. The nonlocal Josephson diode effect requires breaking local time-reversal and local charge-conjugation symmetries, with the latter being unique to minimal Kitaev chains. Our results establish minimal Kitaev chains as a highly controllable platform for engineering nonlocal Josephson phenomena.

Nonlocality is an inherent quantum effect revealing instantaneous action at a distance, tied to the wavefunction nature, and has led to the prediction of several phenomena relevant to quantum technologies [1]. While mostly explored in relation to entanglement [2–4], the concept of nonlocality has been often studied in superconducting devices. Perhaps the simplest example is a two-terminal superconducting junction, where variations of voltages on one terminal give rise to a differential current on the second terminal, thus determining the so-called nonlocal conductance [5–9]. More recently, nonlocality was studied in multi-terminal Josephson junctions, where a supercurrent flows across one part of the system due to variations in the superconducting phases elsewhere, defining what is known as the nonlocal Josephson effect (JE) [10]. Since Josephson junctions are key for superconducting circuits and computing [11–25], the nonlocal JE is directly relevant for quantum applications while offering a way to further delve the foundations of nonlocality.

The research on nonlocal JE has not only attracted theoretical efforts [10, 26–35] but its realization has already been reported in many experiments [36–42]. Most of the studies involved conventional spin-singlet s -wave superconductors, leaving unconventional superconductors seldom explored in spite of their intrinsic nonlocal order parameters. One of the simplest systems that hosts controllable unconventional superconductivity with a p -wave order parameter can be engineered by connecting two quantum dots (QDs) via a superconductor [43, 44]. This setup represents a minimal Kitaev chain, where electron cotunneling (ECT) and crossed Andreev reflections (CARs) mediate superconducting and normal processes between QDs [43, 45]. Minimal Kitaev chains have lately triggered multiple efforts [46–58] and their implementation has already been shown in superconductor-semiconductor hybrids [59–62]. Despite the significant

attention, the nonlocal JE and its impact on minimal Kitaev chains have not yet been studied.

In this work, we consider three laterally coupled minimal Kitaev chains [Fig. 1] and study the emergence of nonlocal Josephson phenomena. In particular, we demonstrate that, when CAR and ECT in the middle minimal Kitaev chain are distinct, an asymmetric phase-dependent Andreev spectrum appears and is controllable by the superconducting phases across the left and right junctions. We find that this asymmetric Andreev spectrum arises from hybridized Andreev bound states at the left and right junctions and requires breaking local time-reversal and local charge-conjugation symmetries. Notably, the asymmetric Andreev spectrum induces a finite supercurrent across one junction by tuning the superconducting phase difference across the other junction, hence unveiling the nonlocal JE. Even more interesting is that the nonlocal supercurrents develop distinct positive and negative critical currents, giving rise to a nonreciprocal Josephson transport that defines the emergence of a non-local Josephson diode effect. We show that this diode

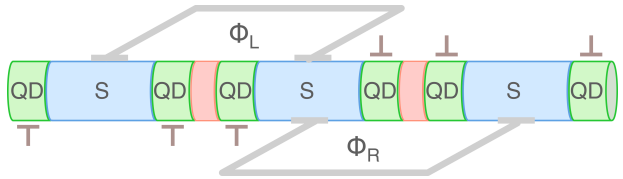


FIG. 1. Three minimal Kitaev chains laterally coupled to form a double Josephson junction, where the phase of the left (right) junction is controlled by an external magnetic flux $\Phi_{L(R)}$. Here, a minimal Kitaev chain is formed by connecting two quantum dots (QDs, green) by a superconductor (S, blue). The onsite energy of the QDs is controlled by gates (bars, brown), while the coupling between minimal Kitaev chains can be tuned by an insulating barrier (red).

effect can achieve robust efficiencies surpassing 50% by controlling CAR and ECT in the middle chain and the phase difference in the second junction. Our findings put forward minimal Kitaev chains for realizing highly tunable nonlocal Josephson phenomena.

JJs formed by three minimal Kitaev chains.—We consider a Josephson system where three minimal Kitaev chains described by

$$H_\alpha(\phi_\alpha) = \varepsilon_{\alpha_1} c_{\alpha_1}^\dagger c_{\alpha_1} + \varepsilon_{\alpha_2} c_{\alpha_2}^\dagger c_{\alpha_2} + t_\alpha c_{\alpha_1}^\dagger c_{\alpha_2} + \Delta_\alpha e^{i\phi_\alpha} c_{\alpha_1}^\dagger c_{\alpha_2}^\dagger + \text{h.c.}$$

are laterally coupled [Fig. 1] and modelled by

$$H(\phi_L, \phi_R) = \sum_\alpha H_\alpha(\phi_\alpha) + \tau_L c_{L_2}^\dagger c_{M_1} + \tau_R c_{M_2}^\dagger c_{R_1} + \text{h.c.} \quad (1)$$

Here $\alpha = L, M, R$ labels the left (L), middle (M), and right (R) minimal Kitaev chains formed by two sites $j = 1, 2$, and c_{α_j} ($c_{\alpha_j}^\dagger$) destroys (creates) an electronic state at site $j = 1, 2$ in the chain α . The first and second terms in $H_\alpha(\phi_\alpha)$ describe onsite energies ε_{α_j} controlled by gates [brown bars in Fig. 1]. The third term represents hopping between sites on the same chain, a characteristic of ECT processes. The fourth term is a spinless superconducting potential, with amplitude Δ_α and phase ϕ_α , describing CAR processes. We model the coupling between the three chains by the second and third terms in Eq. (1) with tunneling amplitudes $\tau_{L(R)}$ across the left (right) junctions. Using a gauge symmetry, we also set the phase of the middle chain as $\phi_M = 0$, leading to the junction depending on two superconducting phases, $H(\phi_L, \phi_R)$. The phase differences ϕ_L and ϕ_R between chains can be externally controlled by magnetic fluxes [Fig. 1], as in Refs. [40, 42, 63]. Despite the simplicity, two-site Kitaev chains have already been experimentally realized in QDs coupled by a superconductor-semiconductor system [59–62, 64], where the control of ECT and CAR was demonstrated [65, 66]. As we show below, the system exhibits a unique phase dependence, enabling a nonlocal JE with nonreciprocal origin.

Breaking and preservation of symmetries.—We begin by analyzing symmetries of the Josephson system in Eq. (1). First of all, the quasi-particle energy derived by Eq. (1) forms a pair $(-E, E)$ because of particle-hole symmetry (PHS) of the Bogoliubov-de Gennes Hamiltonian. While the Josephson system respects time-reversal symmetry (TRS), $\mathcal{T}H(\phi_L, \phi_R)\mathcal{T}^{-1} = H(-\phi_L, -\phi_R)$, where the time-reversal anti-unitary operator \mathcal{T} is given by $\mathcal{T}c_{\alpha_i}\mathcal{T}^{-1} = c_{\alpha_i}$, it does not have either $\mathcal{T}H(\phi_L, \phi_R)\mathcal{T}^{-1} = H(-\phi_L, \phi_R)$ or $\mathcal{T}H(\phi_L, \phi_R)\mathcal{T}^{-1} = H(\phi_L, -\phi_R)$, implying local TRS is broken either across the left or right junctions, respectively. For $\tau_{L(R)} \neq 0$, the left (right) junction also explicitly breaks the local spatial inversion symmetry, even when the entire system may be spatially inversion-symmetric. Thus,

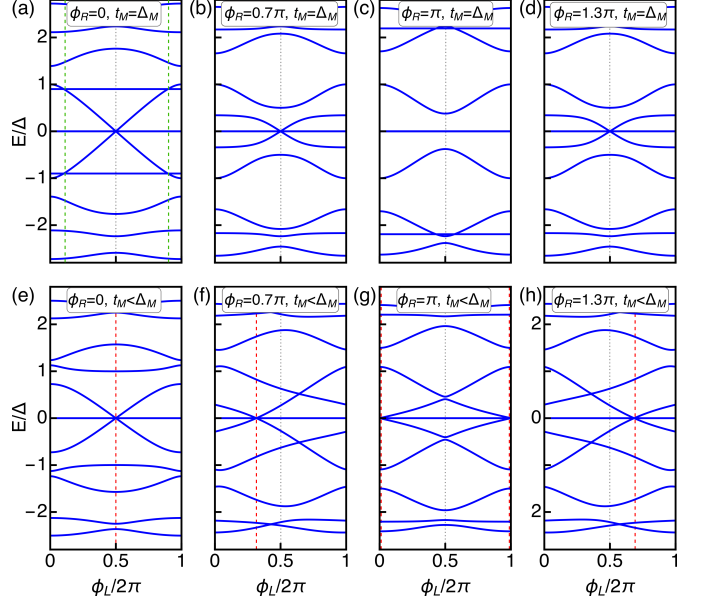


FIG. 2. Energy spectrum as a function of ϕ_L at distinct ϕ_R for $t_M = \Delta_M$ (a-d) and $t_M < \Delta_M$ (e-h). The vertical dotted line marks $\phi_L = \pi$, while the red vertical dashed line marks ϕ_L at which the dispersing lowest ABSs reach zero energy. Parameters: $\varepsilon_\alpha = 0$, $t_{L,R} = \Delta_{L,R} \equiv \Delta = 1$, $\tau_L = 1$, $\tau_R = 0.9$.

each junction satisfies the standard criterion for the Josephson diode effect [67–69]. However, our system Eq. (1) has an additional symmetry constraint for the Josephson diode effect, which originates from a special symmetry at the “sweet spot” ($\varepsilon_\alpha = 0$, $t_\alpha = \Delta_\alpha$), where the chains support quadratically protected Majorana states [43]. In fact, for $\varepsilon_\alpha = 0$ and $t_\alpha = \Delta_\alpha$, each minimal chain has a local charge-conjugation symmetry, $\mathcal{C}_{\alpha_1} H_\alpha(\phi_\alpha) \mathcal{C}_{\alpha_1}^{-1} = H_\alpha(-\phi_\alpha)$, where the non-trivial action of the unitary operator \mathcal{C}_{α_1} is defined by $\mathcal{C}_{\alpha_1} c_{\alpha_1} \mathcal{C}_{\alpha_1}^{-1} = c_{\alpha_1}^\dagger$, $\mathcal{C}_{\alpha_1} c_{\alpha_2} \mathcal{C}_{\alpha_1}^{-1} = -e^{i\phi_\alpha} c_{\alpha_2}$, $\mathcal{C}_{\alpha_1} c_{\beta_i} \mathcal{C}_{\alpha_1}^{-1} = c_{\beta_i}$ ($\beta \neq \alpha$). Note that \mathcal{C}_{α_1} switches only an electron at site 1 on chain α with its antiparticle. We also have a similar local charge-conjugation symmetry \mathcal{C}_{α_2} , switching only an electron at site 2 with its antiparticle. We can partially keep the symmetries even for the junctions in Eq. (1). For instance, by performing \mathcal{C}_{L_2} , \mathcal{C}_{M_1} , and an additional gauge rotation, we have $\mathcal{C}_{LM} H(\phi_L, \phi_R) \mathcal{C}_{LM}^{-1} = H(-\phi_L, \phi_R)$, where the unitary operator \mathcal{C}_{LM} acts as $\mathcal{C}_{LM} c_{L_1} \mathcal{C}_{LM}^{-1} = e^{i\phi_L} c_{L_1}$, $\mathcal{C}_{LM} c_{L_2} \mathcal{C}_{LM}^{-1} = c_{L_2}^\dagger$, $\mathcal{C}_{LM} c_{M_1} \mathcal{C}_{LM}^{-1} = -c_{M_1}^\dagger$, $\mathcal{C}_{LM} c_{M_2} \mathcal{C}_{LM}^{-1} = c_{M_2}$, and $\mathcal{C}_{LM} c_{R_i} \mathcal{C}_{LM}^{-1} = c_{R_i}$. We also have the relation $\mathcal{C}_{MR} H(\phi_L, \phi_R) \mathcal{C}_{MR}^{-1} = H(\phi_L, -\phi_R)$ with an unitary operator \mathcal{C}_{MR} constructed similarly. These relations provide the same constraint on the quasi-particle spectrum as local inversion, $E_n(\phi_L, \phi_R) = E_n(\pm\phi_L, \pm\phi_R)$, and thus, we need to break these local charge-conjugation symmetries, in addition to local TRS, to obtain the Josephson diode effect. For this purpose, we consider $\Delta_M \neq t_M$ below,

which breaks both \mathcal{C}_{LM} and \mathcal{C}_{MR} .

Andreev bound states and Andreev molecules.—Having identified the role of the superconducting phase differences $\phi_{L,R}$ on the system symmetries, here we explore how they determine the behavior of the Andreev energy spectrum. This is shown in Fig. 2(a-d) as a function of ϕ_L when ECT and CAR in the middle chain are the same ($t_M = \Delta_M$) for distinct values of ϕ_R at $\Delta_{L,R} = t_{L,R}$, while in Fig. 2(e-h) for ECT weaker than CAR. Since $\Delta_{L,R} = t_{L,R}$, the left (right) chains host zero-energy dispersionless Majorana flat bands located in their first (second) QD, which remain robust against $\phi_{L,R}$ [Fig. 2]. Depending on the ratio between CAR and ECT in the middle chain, the Andreev spectrum exhibits a strong dependence on $\phi_{L,R}$. For $t_M = \Delta_M$ at $\phi_R = 0$ [Fig. 2(a)], a pair of dispersionless Andreev bound states (ABSs) appear at energies close to $\pm\Delta$ and intersect a pair of dispersing ABSs near $\phi_L = 0, 2\pi$. See green vertical lines. These dispersionless ABSs originate from the right junction between the middle and right chains, and, as ϕ_R takes finite values, they hybridize with the dispersing ABSs formed in the left junction between the left and middle chains [Figs. 2(a-d)]. The dispersing hybridized ABSs, which can be seen as Andreev molecules studied before in conventional superconductors [10, 26, 33, 41, 63, 70–73], reach zero energy at $\phi_L = \pi$ (gray vertical line) and become flat bands with ϕ_L at $\phi_R = \pi$ [Fig. 2(c)], always maintaining a symmetric profile about $\phi_L = \pi$. When $t_M \neq \Delta_M$, a nonzero ϕ_R modifies the phase dependence of the spectrum and, notably, it also makes the spectrum asymmetric about $\phi_L = \pi$ (vertical dashed red line), provided $\phi_R \neq 2\pi n$ with $n \in \mathbb{Z}$; see Fig. 2(e-h) and Fig. 5 in S1 of the End Matter. This asymmetry moves the zero-energy crossing of the dispersing hybridized ABSs to $\phi_L \neq \pi$, which occurs below (above) $\phi_L = \pi$ when $\phi_R < \pi$ ($\phi_R > \pi$) for $t_M < \Delta_M$ [Fig. 2(e-h)]. The asymmetric spectrum turns out to be gapless over $\phi_{L,R} \in (0, 2\pi)$ and remains for $t_M > \Delta_M$ but with the zero-energy crossing at $\phi_L < \pi$ ($\phi_L > \pi$) when $\phi_R > \pi$ ($\phi_R < \pi$) in the latter case [Fig. 5]. A consequence of the asymmetric spectrum under $\phi_{L,R} \neq 0$ and $\Delta_M \neq t_M$ is that the free energy develops minima away from $\phi_L = 2\pi n$, unlike conventional Josephson junctions [74, 75]; (See S1 in End Matter). Thus, the imbalance between CAR and ECT in the middle Kitaev chain induces an asymmetric Andreev spectrum at nonzero superconducting phases across the left/right junctions, in line with breaking local TR and local charge-conjugation symmetries.

Local and nonlocal Josephson effect.—A direct consequence of $\phi_{L,R} \neq 0$ and the imbalance between CAR and ECT in the middle chain is the phase-biased Josephson effect, which we explore here. For this purpose, we numerically obtain the phase-biased Josephson current flowing across the left junction as [24, 76, 77] $I_L(\phi_L, \phi_R) = (e/h) \sum_{n<0} dE_n(\phi_L, \phi_R)/d\phi_L$ [78]. To visualize the supercurrent, in Figs. 3(a,c,e) we show I_L as

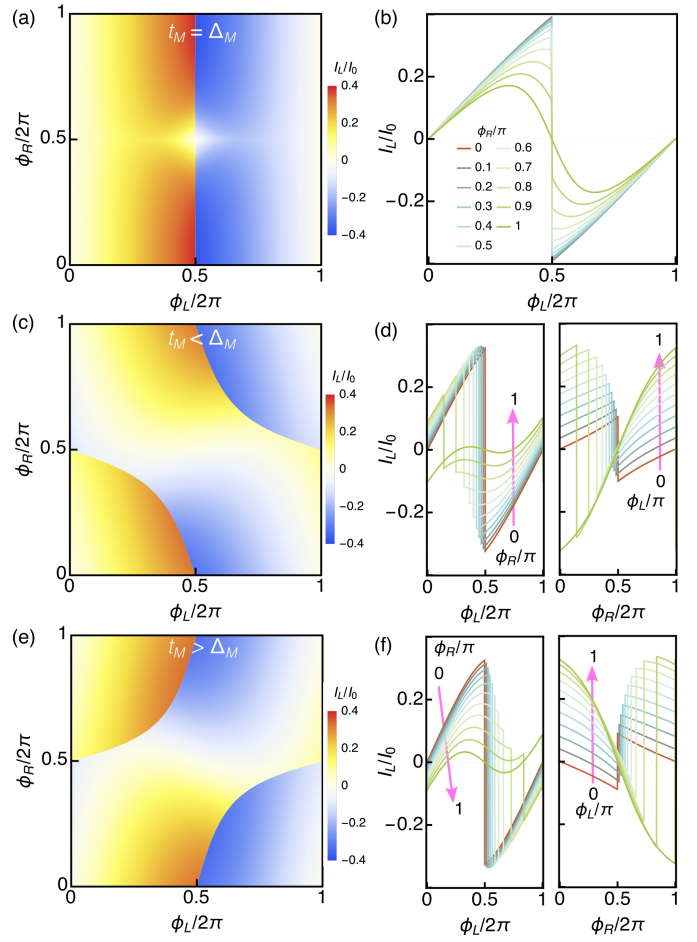


FIG. 3. (a,c,e) Supercurrent as a function of ϕ_L and ϕ_R for $t_M < \Delta_M$ (a), $t_M = \Delta_M$ (c), and $t_M > \Delta_M$ (e). (b,d,f) Line cuts as a function of $\phi_{L(R)}$ for distinct $\phi_{R(L)}$. In (d,f), the magenta arrow indicates variations of $\phi_{L,R}$ within $(0, \pi)$ in steps of 0.1π . Parameters: $I_0 = e\Delta/\hbar$, the rest as in Fig. 2.

a function of ϕ_L and ϕ_R for distinct cases when CAR in the middle chain is equal (a), weaker (c), and stronger (e) than ECT in the same chain. In Figs. 3(b,d,f) we show I_L as a function of ϕ_L for distinct ϕ_R , while Figs. 3(d,f) also show I_L as a function of ϕ_R for distinct ϕ_L . The first observation is that I_L in Figs. 3 strongly depends on $\phi_{L,R}$ and the ratio between ECT (t_M) and CAR (Δ_M) in the middle region, a behavior that originates from the ABSs in Figs. 2. When $\Delta_M = t_M$, the supercurrent I_L is 2π -periodic and symmetric under $\phi_R \neq 0$ [Figs. 3(a,b)], having $I_L(\phi_L = n\pi) = 0$ for any ϕ_R and equal maxima/minima that reduce for $\phi_R \neq 0, 2\pi$; the free energy in Fig. 6(a) has a minimum at ϕ_L as for 0-junctions [74, 79]. Also, I_L exhibits a sawtooth profile at $\phi_L = \pi$ for $\phi_R \neq \pi$ due to the zero-energy crossing of the dispersing ABSs [Figs. 2(a-d)], while it smoothens out at $\phi_R = \pi$ because the dispersing ABSs become flat [Figs. 2(c)].

At $\Delta_M \neq t_M$, the supercurrent across the left junction I_L develops an intriguing anomalous behavior that varies

with $\phi_{L,R} \neq 0$. See Figs. 3(c-f). The most notorious feature is that $\phi_R \neq n\pi$ gives rise to $I_L(\phi_L = n\pi) \neq 0$ with $n \in \mathbb{Z}$ and it is not symmetric about $\phi_L = \pi$ anymore, which are consequences of the asymmetric Andreev spectrum shown in Figs. 2(e-h). This implies that, even at $\phi_L = 0$, a supercurrent across the left junction I_L emerges and is controlled by the superconducting phase difference across the right junction ϕ_R , signalling the so-called nonlocal JE which was initially predicted in systems with conventional superconductors [10]. The sawtooth profile of I_L also occurs away from $\phi_L = \pi$ [Figs. 3(d,f)] due to the shifted zero-energy crossing in the ABSs when $t_M \neq \Delta_M$. See Figs. 2(e-h) and Figs. 5. It is worth noting that, having $I_L(\phi_L = 0, \phi_R \neq n\pi) \neq 0$ in Figs. 3(c-f) also means that a $\phi_{L,0}$ -Josephson junction is realized at $\Delta_M \neq t_M$ [74, 79, 80]. At $\phi_L = 0$, the current as a function of ϕ_R can develop a π -shift for $t_M > \Delta_M$ [Figs. 3(e,f)], leading to a π -junction [79]. Moreover, there are also signals of a ϕ -junction behavior [81–84], where the current I_L passes through zero neither at $\phi_L = 0, 2\pi$ nor $\phi_L = \pi$ [Figs. 3(d,f)]. Yet another important effect of $\phi_{L,R} \neq 0$ and $t_M \neq \Delta_M$ is that the maximum positive and negative values of I_L over $\phi_L \in (0, 2\pi)$ are not the same [Figs. 3(c-f)], producing a nonreciprocity between the maximum currents that can flow across the left junction. As a result, a Josephson setup with three laterally coupled minimal Kitaev chains [Eq. (1)] can realize the nonlocal Josephson effect and nonlocal nonreciprocal Josephson transport only when ECT and CAR in the middle chain are distinct.

Critical currents and nonlocal Josephson diode effect.—To further explore the nonlocal nonreciprocal Josephson transport, we look at the critical currents across the left junction $I_{cL}^\pm(\phi_R) = \max_{\phi_L} [\pm I_L(\phi_L, \phi_R)]$, where $I_L(\phi_L, \phi_R)$ is the current flowing across the left junction discussed in the previous section. Figs. 4(a-c) show the critical currents $I_{cL}^\pm(\phi_R)$ as a function of ϕ_R when ECT in the middle chain is weaker, equal, and stronger than CAR in the same chain. At $t_M = \Delta_M$, when CAR and ECT in the middle chain are distinct, the positive and negative critical currents are equal ($I_{cL}^+(\phi_R) = I_{cL}^-(\phi_R)$) and develop a minimum at $\phi_R = \pi$ [Fig. 4(b)], leading to the absence of the nonlocal Josephson diode effect. Interestingly, for $t_M < \Delta_M$, the minima of $I_{cL}^+(\phi_R)$ and $I_{cL}^-(\phi_R)$ are shifted to values below and above $\phi_R = \pi$, respectively, giving rise to nonreciprocal phase-biased Josephson currents ($I_{cL}^+(\phi_R) \neq I_{cL}^-(\phi_R)$) flowing across the left junction and fully controlled by $\phi_R \neq n\pi$. For $t_M > \Delta_M$, the shifts in the critical currents is the opposite as for $t_M < \Delta_M$ but $I_{cL}^+(\phi_R) \neq I_{cL}^-(\phi_R)$ remains. Having $I_{cL}^+(\phi_R) \neq I_{cL}^-(\phi_R)$ defines the nonlocal Josephson diode effect, which requires an imbalance between CAR and ECT in the middle chain and also $\phi_R \neq n\pi$. These conditions are consistent with the asymmetric Andreev spectrum [Fig. 2] and with the breaking of local TR and charge-conjugation symmetries discussed

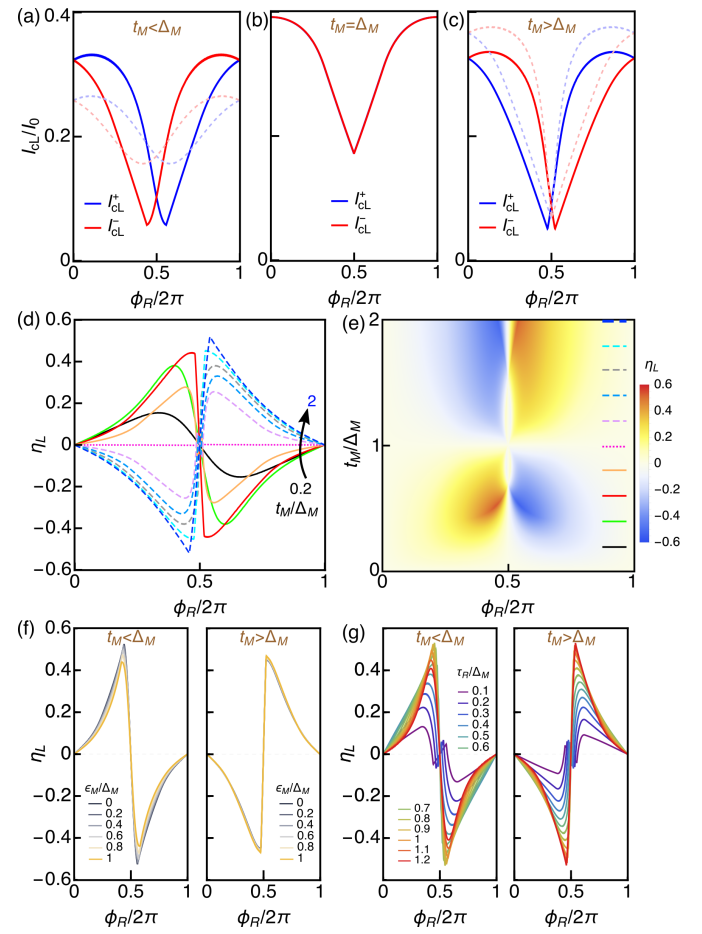


FIG. 4. (a-c) Critical currents I_{cL}^\pm as functions of ϕ_R for $t_M < \Delta_M$ (a), $t_M = \Delta_M$ (b), and $t_M > \Delta_M$ (c). The dashed and solid lines in (a) correspond to $t_M = 0.2\Delta_M$ and $t_M = 0.5\Delta_M$, while to $t_M = 1.5\Delta_M$ and $t_M = 1.8\Delta_M$ in (c). (d,e) Diode's quality factor η_L as a function of ϕ_R for distinct t_M in steps of $0.2\Delta_M$, marked by colored bars in (e). (f) η_L as a function of ϕ_R for distinct ϵ_M for $t_M < \Delta_M$ and $t_M > \Delta_M$. (g) The same as in (f) but for distinct τ_R . Parameters: $I_0 = e\Delta/\hbar$, the rest as in Fig. 2.

below Eq. (1), implying that they are crucial for the nonlocal Josephson diode effect in minimal Kitaev chains.

To characterize the nonlocal diode effect, we analyze its efficiency by studying the quality factor $\eta_L(\phi_R) = [I_{cL}^+(\phi_R) - I_{cL}^-(\phi_R)]/[I_{cL}^+(\phi_R) + I_{cL}^-(\phi_R)]$, where $I_{cL}^\pm(\phi_R)$ are the critical currents across the left junction analyzed in the previous paragraph. We show $\eta_L(\phi_R)$ in Fig. 4(d,e) as a function of ϕ_R and t_M , while in Fig. 4(f,g) we inspect the stability of the efficiencies when varying the onsite energies and tunneling across the junction since these conditions are very likely unavoidable in a realistic scenario. In S3 and Fig. 7 of the End Matter, we discuss the robustness of $\eta_L(\phi_R)$ against variations of the onsite energies ϵ_α . In Fig. 4(d,e), we observe that a nonzero quality factor appears when $t_M \neq \Delta_M$ and $\phi_R \neq n\pi$, with $n \in \mathbb{Z}$, and it is enhanced just below and above

$\phi_R = \pi$ achieving values above 0.5. While $t_M/\Delta_M < 1$ promotes a quality factor having a sine-line profile with ϕ_R with a fast sign change across $\phi_R = \pi$, the quality factors change sign for $t_M/\Delta_M > 1$, see Fig. 4(d,e). This implies that the diode's polarity and large efficiencies can be fully controlled nonlocally by ϕ_R and is thus expected to be more tunable than regular two-terminal Josephson diodes [68, 69, 85–101]. The large efficiencies of the nonlocal Josephson diode effect are robust against variations of the onsite energies of the middle chain, as demonstrated in Figs. 4(f). Strong variations of the onsite energies in the left and right chains, however, have a detrimental effect although $\eta_L(\phi_R)$ remains robust against weak detuning, see Fig. 7. Moreover, having large tunneling amplitudes favours the large efficiency values of the nonlocal Josephson diode [Fig. 4(g)]. We have also verified that slight deviations from the equal CAR and ECT regime in the left /right chains weakly affects the nonlocal Josephson diode effect.

In conclusion, we have demonstrated the nonlocal Josephson effect and the realization of a nonlocal Josephson diode in a system formed by three laterally coupled minimal Kitaev chains. In particular, we found that when the middle chain exhibits an imbalance between crossed Andreev reflections and electron cotunneling, the phase-dependent Andreev spectrum is asymmetric and can be controlled by the phase difference across the right junction. We have then shown that this asymmetric Andreev spectrum, containing hybridized Andreev bound states from both junctions, produces a supercurrent across the left junction that is controllable by the phase difference across the right junction, hence defining the nonlocal Josephson effect. Notably, we have discovered that these nonlocal Josephson effects enable distinct positive and negative critical currents, giving rise to a nonlocal Josephson diode effect whose polarity is highly tunable and can achieve efficiencies above 50%. Given the recent advances on nonlocal Josephson effect [36–42] and minimal Kitaev chains [59–62], our findings are very likely within experimental reach.

J. C. acknowledges financial support from the Swedish Research Council (Vetenskapsrådet Grant No. 2021-04121). M. S. was supported by JST CREST Grant No. JPMJCR19T2 and JSPS KAKENHI Grant Nos. JP24K00569 and JP25H01250.

Commun. **2**, 184 (2011).

- [4] L. Villegas-Aguilar, E. Polino, F. Ghafari, M. T. Quintino, K. T. Laverick, I. R. Berkman, S. Rogge, L. K. Shalm, N. Tischler, E. G. Cavalcanti, *et al.*, Nonlocality activation in a photonic quantum network, Nat. Commun. **15**, 3112 (2024).
- [5] A. Pöschl, A. Danilenko, D. Sabonis, K. Kristjuhan, T. Lindemann, C. Thomas, M. J. Manfra, and C. M. Marcus, Nonlocal conductance spectroscopy of Andreev bound states in gate-defined inas/al nanowires, Phys. Rev. B **106**, L241301 (2022).
- [6] J. Danon, A. B. Hellenes, E. B. Hansen, L. Casparis, A. P. Higginbotham, and K. Flensberg, Nonlocal conductance spectroscopy of Andreev bound states: Symmetry relations and BCS charges, Phys. Rev. Lett. **124**, 036801 (2020).
- [7] J. Feng, H. F. Legg, M. Bagchi, D. Loss, J. Klinovaja, and Y. Ando, Long-range crossed Andreev reflection in a topological insulator nanowire proximitized by a superconductor, Nat. Phys. **21**, 708 (2025).
- [8] H. Zhang, D. E. Liu, M. Wimmer, and L. P. Kouwenhoven, Next steps of quantum transport in majorana nanowire devices, Nat. Commun. **10**, 1 (2019).
- [9] S. M. Frolov, M. J. Manfra, and J. D. Sau, Topological superconductivity in hybrid devices, Nat. Phys. **16**, 718 (2020).
- [10] J.-D. Pillet, V. Benzoni, J. Griesmar, J.-L. Smirr, and c. O. Girit, Nonlocal Josephson effect in Andreev molecules, Nano Letters **19**, 7138 (2019).
- [11] M. H. Devoret, A. Wallraff, and J. M. Martinis, Superconducting qubits: A short review (2004), arXiv:cond-mat/0411174 [cond-mat.mes-hall].
- [12] J. Clarke and F. K. Wilhelm, Superconducting quantum bits, Nature **453**, 1031 (2008).
- [13] T. Brecht, W. Pfaff, C. Wang, Y. Chu, L. Frunzio, M. H. Devoret, and R. J. Schoelkopf, Multilayer microwave integrated quantum circuits for scalable quantum computing, npj Quantum Inf. **2**, 16002 (2016).
- [14] P. Krantz, M. Kjaergaard, F. Yan, T. P. Orlando, S. Gustavsson, and W. D. Oliver, A quantum engineer's guide to superconducting qubits, Appl. Phys. Rev. **6**, 021318 (2019).
- [15] J. M. Martinis, M. H. Devoret, and J. Clarke, Quantum Josephson junction circuits and the dawn of artificial atoms, Nat. Phys. **16**, 234 (2020).
- [16] R. Aguado, A perspective on semiconductor-based superconducting qubits, Appl. Phys. Lett. **117** (2020).
- [17] M. Benito and G. Burkard, Hybrid superconductor-semiconductor systems for quantum technology, Applied Physics Letters **116**, 190502 (2020).
- [18] R. Aguado and L. P. Kouwenhoven, Majorana qubits for topological quantum computing, Phys. Today. **73**, 44 (2020).
- [19] S. Rasmussen, K. Christensen, S. Pedersen, L. Kristensen, T. Bækkegaard, N. Loft, and N. Zinner, Superconducting circuit companion—an introduction with worked examples, PRX Quantum **2**, 040204 (2021).
- [20] I. Siddiqi, Engineering high-coherence superconducting qubits, Nat. Rev. Mater. **6**, 875 (2021).
- [21] A. Bargerbos, M. Pita-Vidal, R. Žitko, J. Ávila, L. J. Splitthoff, L. Grünhaupt, J. J. Wesdorp, C. K. Andersen, Y. Liu, L. P. Kouwenhoven, R. Aguado, A. Kou, and B. van Heck, Singlet-doublet transitions of a quan-

-
- [1] N. Brunner, D. Cavalcanti, S. Pironio, V. Scarani, and S. Wehner, Bell nonlocality, Rev. Mod. Phys. **86**, 419 (2014).
 - [2] H. Buhrman, R. Cleve, S. Massar, and R. de Wolf, Nonlocality and communication complexity, Rev. Mod. Phys. **82**, 665 (2010).
 - [3] D. Cavalcanti, M. L. Almeida, V. Scarani, and A. Acin, Quantum networks reveal quantum nonlocality, Nat.

- tum dot josephson junction detected in a transmon circuit, PRX Quantum **3**, 030311 (2022).
- [22] M. Kjaergaard, M. E. Schwartz, J. Braumüller, P. Krantz, J. I.-J. Wang, S. Gustavsson, and W. D. Oliver, Superconducting qubits: Current state of play, Annu. Rev. Condens. Matter Phys. **11**, 369 (2020).
- [23] M. Pita-Vidal, A. Bargerbos, R. Žitko, L. J. Splitthoff, L. Grünhaupt, J. J. Wesdorp, Y. Liu, L. P. Kouwenhoven, R. Aguado, B. van Heck, *et al.*, Direct manipulation of a superconducting spin qubit strongly coupled to a transmon qubit, Nat. Phys. **19**, 1110 (2023).
- [24] Y. Tanaka, S. Tamura, and J. Cayao, Theory of Majorana zero modes in unconventional superconductors, Prog. Theor. Exp. Phys. **2024**, 08C105 (2024).
- [25] Y. Fukaya, B. Lu, K. Yada, Y. Tanaka, and J. Cayao, Superconducting phenomena in systems with unconventional magnets, J. Phys.: Condens. Matter **37**, 313003 (2025).
- [26] J.-D. Pillet, V. Benzoni, J. Griesmar, J.-L. Smirr, and Çağlar Ö. Girit, Scattering description of Andreev molecules, SciPost Phys. Core **2**, 009 (2020).
- [27] H.-Y. Xie, M. G. Vavilov, and A. Levchenko, Weyl nodes in Andreev spectra of multiterminal Josephson junctions: Chern numbers, conductances, and supercurrents, Phys. Rev. B **97**, 035443 (2018).
- [28] R. Mélin, Inversion in a four-terminal superconducting device on the quartet line. i. two-dimensional metal and the quartet beam splitter, Phys. Rev. B **102**, 245435 (2020).
- [29] R. Mélin, Ultralong-distance quantum correlations in three-terminal Josephson junctions, Phys. Rev. B **104**, 075402 (2021).
- [30] J. Cayao, P. Burset, and Y. Tanaka, Controllable odd-frequency Cooper pairs in multisuperconductor Josephson junctions, Phys. Rev. B **109**, 205406 (2024).
- [31] J. H. Correa and M. P. Nowak, Theory of universal diode effect in three-terminal Josephson junctions, SciPost Phys. **17**, 037 (2024).
- [32] J.-D. Pillet, S. Annabi, A. Peugeot, H. Riechert, E. Arribi, J. Griesmar, and L. Bretheau, Josephson diode effect in Andreev molecules, Phys. Rev. Res. **5**, 033199 (2023).
- [33] F. Matute-Cañadas, L. Tosi, and A. L. Yeyati, Quantum circuits with multiterminal Josephson-Andreev junctions, PRX Quantum **5**, 020340 (2024).
- [34] J. Cayao and M. Sato, Non-Hermitian multiterminal phase-biased Josephson junctions, Phys. Rev. B **110**, 235426 (2024).
- [35] G. A. Bobkov, D. S. Rabinovich, A. M. Bobkov, and I. V. Bobkova, Gate-tunable nonlocal Josephson effect through magnetic van der Waals bilayers, Phys. Rev. B **111**, 024506 (2025).
- [36] E. Strambini, S. D'ambrosio, F. Vischi, F. Bergeret, Y. V. Nazarov, and F. Giavotto, The ω -squirt as a tool to phase-engineer Josephson topological materials, Nat. Nanotech. **11**, 1055 (2016).
- [37] N. Pankratova, H. Lee, R. Kuzmin, K. Wickramasinghe, W. Mayer, J. Yuan, M. G. Vavilov, J. Shabani, and V. E. Manucharyan, Multiterminal Josephson effect, Phys. Rev. X **10**, 031051 (2020).
- [38] A. W. Draelos, M.-T. Wei, A. Seredinski, H. Li, Y. Mehta, K. Watanabe, T. Taniguchi, I. V. Borzenets, F. Amet, and G. Finkelstein, Supercurrent flow in multi-terminal graphene Josephson junctions, Nano Lett. **19**, 1039 (2019).
- [39] G. V. Graziano, M. Gupta, M. Pendharkar, J. T. Dong, C. P. Dempsey, C. Palmstrøm, and V. S. Pribiag, Selective control of conductance modes in multi-terminal Josephson junctions, Nat. Commun. **13**, 5933 (2022).
- [40] S. Matsuo, J. S. Lee, C.-Y. Chang, Y. Sato, K. Ueda, C. J. Palmstrøm, and S. Tarucha, Observation of non-local Josephson effect on double InAs nanowires, Commun. Phys. **5**, 221 (2022).
- [41] S. Matsuo, T. Imoto, T. Yokoyama, Y. Sato, T. Lindemann, S. Gronin, G. C. Gardner, M. J. Manfra, and S. Tarucha, Phase engineering of anomalous Josephson effect derived from Andreev molecules, Sci. Adv. **9**, eadj3698 (2023).
- [42] D. Z. Haxell, M. Coraiola, M. Hinderling, S. C. ten Kate, D. Sabonis, A. E. Svetogorov, W. Belzig, E. Cheah, F. Krizek, R. Schott, W. Wegscheider, and F. Nicelle, Demonstration of the nonlocal Josephson effect in Andreev molecules, Nano Letters **23**, 7532 (2023).
- [43] M. Leijnse and K. Flensberg, Parity qubits and poor man's Majorana bound states in double quantum dots, Phys. Rev. B **86**, 134528 (2012).
- [44] B. Sothmann, S. Weiss, M. Governale, and J. König, Unconventional superconductivity in double quantum dots, Phys. Rev. B **90**, 220501 (2014).
- [45] J. D. Sau and S. D. Sarma, Realizing a robust practical majorana chain in a quantum-dot-superconductor linear array, Nat. Commun. **3**, 964 (2012).
- [46] A. Tsintzis, R. S. Souto, and M. Leijnse, Creating and detecting poor man's majorana bound states in interacting quantum dots, Phys. Rev. B **106**, L201404 (2022).
- [47] A. Tsintzis, R. S. Souto, K. Flensberg, J. Danon, and M. Leijnse, Majorana qubits and non-Abelian physics in quantum dot-based minimal Kitaev chains, PRX Quantum **5**, 010323 (2024).
- [48] R. Seoane Souto, A. Tsintzis, M. Leijnse, and J. Danon, Probing Majorana localization in minimal Kitaev chains through a quantum dot, Phys. Rev. Res. **5**, 043182 (2023).
- [49] J. Cayao, Emergent pair symmetries in systems with poor man's Majorana modes, Phys. Rev. B **110**, 125408 (2024).
- [50] J. Cayao and R. Aguado, Non-Hermitian minimal Kitaev chains, Phys. Rev. B **111**, 205432 (2025).
- [51] C.-X. Liu, A. M. Bozkurt, F. Zatelli, S. L. ten Haaf, T. Dvir, and M. Wimmer, Enhancing the excitation gap of a quantum-dot-based Kitaev chain, Commun. Phys. **7**, 235 (2024).
- [52] M. Alvarado, A. L. Yeyati, R. Aguado, and R. S. Souto, Interplay between Majorana and Shiba states in a minimal Kitaev chain coupled to a superconductor, Phys. Rev. B **110**, 245144 (2024).
- [53] W. Samuelson, V. Svensson, and M. Leijnse, Minimal quantum dot based Kitaev chain with only local superconducting proximity effect, Phys. Rev. B **109**, 035415 (2024).
- [54] O. A. Awoga and J. Cayao, Identifying trivial and majorana zero-energy modes using the majorana polarization, Phys. Rev. B **110**, 165404 (2024).
- [55] M. Luethi, H. F. Legg, D. Loss, and J. Klinovaja, From perfect to imperfect poor man's Majoranas in minimal Kitaev chains, Phys. Rev. B **110**, 245412 (2024).
- [56] M. Luethi, H. F. Legg, D. Loss, and J. Klinovaja, Fate

- of poor man's Majoranas in the long Kitaev chain limit, Phys. Rev. B **111**, 115419 (2025).
- [57] M. Nitsch, L. Maffi, V. V. Baran, R. S. Souto, J. Paaske, M. Leijnse, and M. Burrello, The poor man's majorana tетron, arXiv:2411.11981 (2024).
- [58] V. K. Vimal and J. Cayao, Entanglement dynamics in minimal Kitaev chains, arXiv: 2507.17586 (2025).
- [59] T. Dvir, G. Wang, N. van Loo, C.-X. Liu, G. P. Mazur, A. Bordin, S. L. Ten Haaf, J.-Y. Wang, D. van Driel, F. Zatelli, *et al.*, Realization of a minimal Kitaev chain in coupled quantum dots, Nature **614**, 445 (2023).
- [60] A. Bordin, X. Li, D. van Driel, J. C. Wolff, Q. Wang, S. L. D. ten Haaf, G. Wang, N. van Loo, L. P. Kouwenhoven, and T. Dvir, Crossed andreev reflection and elastic cotunneling in three quantum dots coupled by superconductors, Phys. Rev. Lett. **132**, 056602 (2024).
- [61] A. Bordin, G. Wang, C.-X. Liu, S. L. D. ten Haaf, N. van Loo, G. P. Mazur, D. Xu, D. van Driel, F. Zatelli, S. Gazibegovic, G. Badawy, E. P. A. M. Bakkers, M. Wimmer, L. P. Kouwenhoven, and T. Dvir, Tunable crossed Andreev reflection and elastic cotunneling in hybrid nanowires, Phys. Rev. X **13**, 031031 (2023).
- [62] F. Zatelli, D. van Driel, D. Xu, G. Wang, C.-X. Liu, A. Bordin, B. Roovers, G. P. Mazur, N. van Loo, J. C. Wolff, A. M. Bozkurt, G. Badawy, S. Gazibegovic, E. P. A. M. Bakkers, M. Wimmer, L. P. Kouwenhoven, and T. Dvir, Robust poor man's Majorana zero modes using Yu-Shiba-Rusinov states, arXiv:2311.03193 (2023).
- [63] M. Coraiola, D. Z. Haxell, D. Sabonis, H. Weisbrich, A. E. Svetogorov, M. Hinderling, S. C. ten Kate, E. Cheah, F. Krizek, R. Schott, W. Wegscheider, J. C. Cuevas, W. Belzig, and F. Nichele, Phase-engineering the Andreev band structure of a three-terminal Josephson junction, Nat. Commun. **14**, 6784 (2023).
- [64] S. L. D. ten Haaf, Q. Wang, A. M. Bozkurt, C.-X. Liu, I. Kulesh, P. Kim, D. Xiao, C. Thomas, M. J. Manfra, T. Dvir, M. Wimmer, and S. Goswami, A two-site Kitaev chain in a two-dimensional electron gas, Nature **630**, 329 (2024).
- [65] G. Wang, T. Dvir, G. P. Mazur, C.-X. Liu, N. van Loo, S. L. D. ten Haaf, A. Bordin, S. Gazibegovic, G. Badawy, E. P. A. M. Bakkers, M. Wimmer, and L. P. Kouwenhoven, Singlet and triplet Cooper pair splitting in hybrid superconducting nanowires, Nature **612**, 448 (2022).
- [66] Q. Wang, S. L. D. ten Haaf, I. Kulesh, D. Xiao, C. Thomas, M. J. Manfra, and S. Goswami, Triplet correlations in Cooper pair splitters realized in a two-dimensional electron gas, Nat. Commun. **14**, 4876 (2023).
- [67] J. J. He, Y. Tanaka, and N. Nagaosa, A phenomenological theory of superconductor diodes, New J. Phys. **24**, 053014 (2022).
- [68] B. Lu, S. Ikegaya, P. Burset, Y. Tanaka, and N. Nagaosa, Tunable Josephson diode effect on the surface of topological insulators, Phys. Rev. Lett. **131**, 096001 (2023).
- [69] J. Cayao, N. Nagaosa, and Y. Tanaka, Enhancing the Josephson diode effect with Majorana bound states, Phys. Rev. B **109**, L081405 (2024).
- [70] V. Kornich, H. S. Barakov, and Y. V. Nazarov, Fine energy splitting of overlapping Andreev bound states in multiterminal superconducting nanostructures, Phys. Rev. Res. **1**, 033004 (2019).
- [71] Z. Su, A. B. Tacla, M. Hocevar, D. Car, S. R. Plissard, E. P. A. M. Bakkers, A. J. Daley, D. Pekker, and S. M. Frolov, Andreev molecules in semiconductor nanowire double quantum dots, Nat. Commun. **8**, 585 (2017).
- [72] K. Sakurai, M. T. Mercaldo, S. Kobayashi, A. Yamakage, S. Ikegaya, T. Habe, P. Kotetes, M. Cuoco, and Y. Asano, Nodal Andreev spectra in multi-Majorana three-terminal Josephson junctions, Phys. Rev. B **101**, 174506 (2020).
- [73] S. Matsuo, T. Imoto, T. Yokoyama, Y. Sato, T. Lindemann, S. Gronin, G. C. Gardner, S. Nakosai, Y. Tanaka, M. J. Manfra, *et al.*, Phase-dependent Andreev molecules and superconducting gap closing in coherently-coupled Josephson junctions, Nat. Commun. **14**, 8271 (2023).
- [74] A. A. Golubov, M. Y. Kupriyanov, and E. Il'ichev, The current-phase relation in josephson junctions, Rev. Mod. Phys. **76**, 411 (2004).
- [75] J. Sauls, Andreev bound states and their signatures, Philosophical Transactions of the Royal Society A: Mathematical, Physical and Engineering Sciences **376**, 20180140 (2018).
- [76] C. Beenakker, Three "universal" mesoscopic Josephson effects, in *Transport phenomena in mesoscopic systems: Proceedings of the 14th Taniguchi symposium, Shima, Japan, November 10-14, 1991*, Vol. 109 (Springer-Verlag, 1992) p. 235.
- [77] A. Zagorskin, *Quantum Theory of Many-Body Systems: Techniques and Applications* (Springer, 2014).
- [78] Similarly, we can obtain the supercurrent flowing across the right junction as $I_R(\phi_L, \phi_R) = (e/\hbar) \sum_{n<0} dE_n(\phi_L, \phi_R)/d\phi_R$. We have verified that $I_{L,R}(\phi_L, \phi_R)$ can also be obtained within a Green's function approach [77, 102], but obtaining them from the spectrum offers a direct way to identify the contributing states [103–109].
- [79] A. I. Buzdin, Proximity effects in superconductor-ferromagnet heterostructures, Rev. Mod. Phys. **77**, 935 (2005).
- [80] A. Buzdin, Direct coupling between magnetism and superconducting current in the josephson φ_0 junction, Phys. Rev. Lett. **101**, 107005 (2008).
- [81] R. G. Mints, Self-generated flux in josephson junctions with alternating critical current density, Phys. Rev. B **57**, R3221 (1998).
- [82] A. Buzdin and A. E. Koshelev, Periodic alternating 0- and π -junction structures as realization of φ -josephson junctions, Phys. Rev. B **67**, 220504 (2003).
- [83] B. Lu, K. Maeda, H. Ito, K. Yada, and Y. Tanaka, φ Josephson junction induced by altermagnetism, Phys. Rev. Lett. **133**, 226002 (2024).
- [84] Y. Fukaya, K. Maeda, K. Yada, J. Cayao, Y. Tanaka, and B. Lu, Josephson effect and odd-frequency pairing in superconducting junctions with unconventional magnets, Phys. Rev. B **111**, 064502 (2025).
- [85] J. Hu, C. Wu, and X. Dai, Proposed design of a Josephson diode, Phys. Rev. Lett. **99**, 067004 (2007).
- [86] K. N. Nesterov, M. Houzet, and J. S. Meyer, Anomalous Josephson effect in semiconducting nanowires as a signature of the topologically nontrivial phase, Phys. Rev. B **93**, 174502 (2016).
- [87] F. Dolcini, M. Houzet, and J. S. Meyer, Topological Josephson φ_0 junctions, Phys. Rev. B **92**, 035428 (2015).
- [88] K. Misaki and N. Nagaosa, Theory of the nonreciprocal

- Josephson effect, Phys. Rev. B **103**, 245302 (2021).
- [89] Y. Tanaka, B. Lu, and N. Nagaosa, Theory of giant diode effect in *d*-wave superconductor junctions on the surface of a topological insulator, Phys. Rev. B **106**, 214524 (2022).
- [90] A. Costa, J. Fabian, and D. Kochan, Microscopic study of the Josephson supercurrent diode effect in Josephson junctions based on two-dimensional electron gas, Phys. Rev. B **108**, 054522 (2023).
- [91] R. S. Souto, M. Leijnse, and C. Schrade, Josephson diode effect in supercurrent interferometers, Phys. Rev. Lett. **129**, 267702 (2022).
- [92] S. Mondal, P.-H. Fu, and J. Cayao, Josephson diode effect with Andreev and Majorana bound states, Phys. Rev. B **112**, 144506 (2025).
- [93] Z. Liu, L. Huang, and J. Wang, Josephson diode effect in topological superconductors, Phys. Rev. B **110**, 014519 (2024).
- [94] S. Fracassi, S. Traverso, N. Traverso Ziani, M. Carrega, S. Heun, and M. Sassetti, Anomalous supercurrent and diode effect in locally perturbed topological Josephson junctions, App. Phys. Lett. **124**, 242601 (2024).
- [95] A. Maiani, K. Flensberg, M. Leijnse, C. Schrade, S. Vaitiekėnas, and R. Seoane Souto, Nonsinusoidal current-phase relations in semiconductor-superconductor-ferromagnetic insulator devices, Phys. Rev. B **107**, 245415 (2023).
- [96] M. Davydova, S. Prembabu, and L. Fu, Universal Josephson diode effect, Sci. Adv. **8**, eab00309 (2022).
- [97] H. F. Legg, K. Laubscher, D. Loss, and J. Klinovaja, Parity-protected superconducting diode effect in topological Josephson junctions, Phys. Rev. B **108**, 214520 (2023).
- [98] P.-H. Fu, Y. Xu, S. A. Yang, C. H. Lee, Y. S. Ang, and J.-F. Liu, Field-effect Josephson diode via asymmetric spin-momentum locking states, Phys. Rev. Appl. **21**, 054057 (2024).
- [99] J. S. Meyer and M. Houzet, Josephson diode effect in a ballistic single-channel nanowire, Applied Physics Letters **125**, 022603 (2024).
- [100] J. J. Cuozzo, W. Pan, J. Shabani, and E. Rossi, Microwave-tunable diode effect in asymmetric SQUIDs with topological Josephson junctions, Phys. Rev. Res. **6**, 023011 (2024).
- [101] D. Debnath and P. Dutta, Gate-tunable Josephson diode effect in Rashba spin-orbit coupled quantum dot junctions, Phys. Rev. B **109**, 174511 (2024).
- [102] P. San-Jose, J. Cayao, E. Prada, and R. Aguado, Multiple Andreev reflection and critical current in topological superconducting nanowire junctions, New J. Phys. **15**, 075019 (2013).
- [103] A. Furusaki and M. Tsukada, Dc Josephson effect and Andreev reflection, Solid State Commun. **78**, 299 (1991).
- [104] A. Furusaki, Josephson current carried by Andreev levels in superconducting quantum point contacts, Superlattices and Microstructures **25**, 809 (1999).
- [105] S. Kashiwaya and Y. Tanaka, Tunnelling effects on surface bound states in unconventional superconductors, Rep. Prog. Phys. **63**, 1641 (2000).
- [106] J. Cayao, A. M. Black-Schaffer, E. Prada, and R. Aguado, Andreev spectrum and supercurrents in nanowire-based SNS junctions containing Majorana bound states, Beilstein J. Nanotechnol. **9**, 1339 (2018).
- [107] J. Cayao, P. San-Jose, A. M. Black-Schaffer, R. Aguado, and E. Prada, Majorana splitting from critical currents in Josephson junctions, Phys. Rev. B **96**, 205425 (2017).
- [108] J. Cayao and A. M. Black-Schaffer, Distinguishing trivial and topological zero-energy states in long nanowire junctions, Phys. Rev. B **104**, L020501 (2021).
- [109] O. A. Awoga, J. Cayao, and A. M. Black-Schaffer, Supercurrent detection of topologically trivial zero-energy states in nanowire junctions, Phys. Rev. Lett. **123**, 117001 (2019).

END MATTER

S1. Andreev bound states when ECT is stronger than CAR in the middle chain.—In Fig. 2 we looked at the Andreev spectrum when ECT is equal to or weaker than CAR in the middle chain. In this part, Fig. 5 shows the Andreev spectrum as a function of ϕ_L for distinct ϕ_R when ECT is stronger than CAR, namely, $t_M > \Delta_M$. The Andreev spectrum is symmetric when $\phi_R = 0$ [Fig. 5(a)], developing a phase dependence similar to the case with $t_M < \Delta_M$ in Fig. 2(a). Because we chose $\Delta_{L,R} = t_{L,R}$ and ε_α , the spectrum contains two dispersionless levels at zero energy, which represent the two poor man's Majorana modes located at the very outer QDs. Two extra Andreev bound states reach zero energy at $\phi = \pi$ marked by a vertical dashed red line, and those are located in the middle of the junction. However, deviations from these parameters do not change the symmetric nature of the spectrum in Fig. 5(a) unless $\phi_R \neq n\pi$. This is demonstrated in Fig. 5(b-d), where a $\phi_R \neq n\pi$ makes the entire Andreev spectrum asymmetric with respect to $\phi_L = \pi$, see vertical dashed gray line. The zero-energy crossing seen at $\phi_L = 0$ in Fig. 5(a) shifts to $\phi_L > \pi$ when $\phi_R < \pi$ [Fig. 5(b)], while to $\phi_L < \pi$ for $\phi_R > \pi$ [Fig. 5(d)], see vertical dashed red lines. At $\phi_R = \pi$, the Andreev spectrum is symmetric, the pair of dispersionless levels remain, but the first excited levels now reach zero energy at $\phi_L = 2n\pi$ while leaving a large zero energy splitting at $\phi_L = n\pi$, Fig. 5(c). In conclusion, the asymmetry in the Andreev spectrum is controlled by ϕ_R and $\Delta_M \neq t_M$, in line with the breaking local time-reversal and local charge-conjugation symmetries discussed in the main text.

S2. Free energy of the Josephson setup.—The asymmetric Andreev spectrum showed in the previous section has a direct effect on the free energy, which we discuss in this part. We define a normalized free energy as $\bar{F} = (F - F_{\min})/(F_{\max} - F_{\min})$, where $F_{\max} = \max_{\phi_L} [F(\phi_L, \phi_R)]$ and $F_{\min} = \min_{\phi_L} [F(\phi_L, \phi_R)]$, where the maximum and minimum are obtained over a period of 2π . In Fig. 6, we show \bar{F} as a function of ϕ_L for distinct values of ϕ_R when ECT in the middle chain t_M is equal, weaker, and stronger than CAR in the same chain Δ_M . As anticipated, for $t_M = \Delta_M$ in Fig. 6(a), the free energy \bar{F} develops minima at multiples of $2n\pi$, with $n \in \mathbb{Z}$, irrespective of the values of ϕ_R . This signals a regular Josephson junction behavior. Interestingly, for $t_M \neq \Delta_M$ and $\phi_R \neq 0$, the free energy exhibits minima away from $\phi_L = 2n\pi$, see Fig. 6(b,c). For instance, for $\phi_R = \pi$ at $t_M \neq \Delta_M$, the free energy has two (double) minima away from $\phi_L = 0, \pi$, signaling the emergence of a ϕ -Josephson junction. We note that ϕ -Josephson junctions were initially predicted in Josephson junctions with alternating critical current density [81], in periodic arrays of 0- and π -Josephson junctions [82], and more recently in alter-

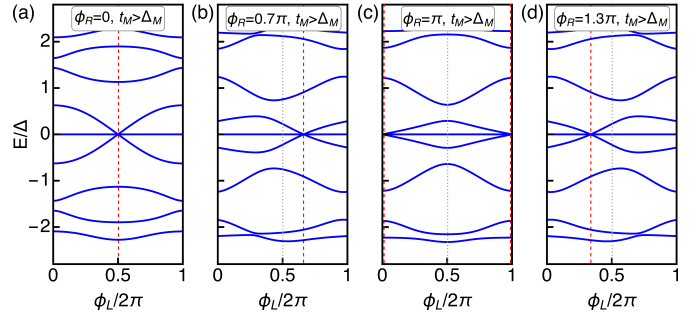


FIG. 5. Energy spectrum as a function of ϕ_L at distinct values of ϕ_R for $t_M = 1.8\Delta_M$. The vertical dotted line marks $\phi_L = \pi$, while the red vertical dashed line marks the value of ϕ_L at which the dispersing lowest ABSs reach zero energy. Parameters: $\varepsilon_\alpha = 0$, $t_{L,R} = \Delta_\alpha \equiv \Delta = 1$, $\tau_L = 1$, $\tau_R = 0.9$.

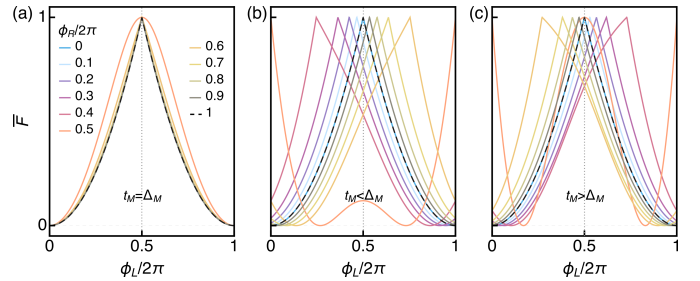


FIG. 6. Free energy \bar{F} as a function of ϕ_L at distinct values of ϕ_R for $t_M = \Delta_M$, $t_M = 0.5\Delta_M$, and $t_M = 1.8\Delta_M$. Here, \bar{F} is defined as $\bar{F} = (F - F_{\min})/(F_{\max} - F_{\min})$, where F is the free energy and $F_{\max(\min)}$ is the maximum (minimum) free energy value over a period of ϕ_L . Parameters: $\varepsilon_\alpha = 0$, $t_{L,R} = \Delta_\alpha \equiv \Delta = 1$, $\tau_L = 1$, $\tau_R = 0.9$.

magnetic Josephson junctions [25, 83, 84]. Furthermore, away from $\phi_R = \pi$ at $t_M \neq \Delta_M$, the free energy is able to exhibit one minimum either close to $\phi_L = 0$ or $\phi_L = 2\pi$: on one hand, when $\pi < \phi_R < 2\pi$, the minimum is close to $\phi_L = 0$ for $t_M < \Delta_M$ but close to $\phi_L = 2n\pi$ for $t_M > \Delta_M$. On the other hand, when $0 < \phi_R < \pi$, the minimum is close to $\phi_L = 2\pi$ for $t_M < \Delta_M$ but close to $\phi_L = 0$ for $t_M > \Delta_M$. The asymmetric Andreev spectrum and non-reciprocal (diode) Josephson transport discussed in the main text is therefore tied to the free energy having a single minimum away from $\phi_L = 2n\pi$.

S3. Efficiency of the nonlocal Josephson diode at finite onsite energies.—To further support the robustness of the nonlocal Josephson diode effect presented in Fig. 4, here we explore the sensitivity of the quality factor η_L under variations of the onsite energies ε_α . This is presented in Fig. 7(a,b), where we show η_L as a function of ϕ_R when the onsite energies of the first QD of the left and right chains take finite values, while in Fig. 7(b,c) we consider the case when both onsite energies of the left and right

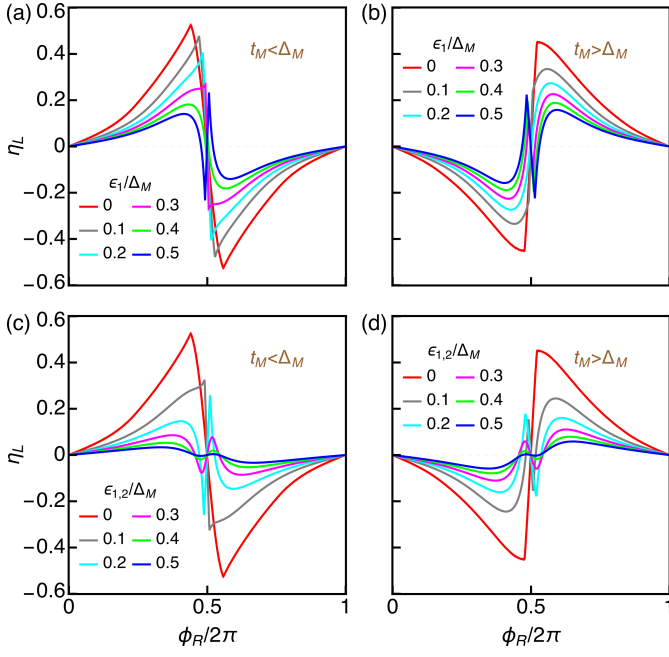


FIG. 7. (a,b) Diode's efficiency as a function of ϕ_R for distinct values of the onsite energy $\epsilon_{L_1,R_1} = \epsilon_1$ when $t_M = 0.5\Delta_M$ (a) and $t_M = 1.8\Delta_M$ (a), in both cases at $\epsilon_{L_2(R_2)} = 0$. (c,d) The same as in (a,b) but both onsite energies $\epsilon_{L_{1,2}} = \epsilon_{R_{1,2}} = \epsilon_{1,2}$. Parameters: $\epsilon_M = 0$, $t_{L,R} = \Delta_\alpha \equiv \Delta = 1$, $\tau_L = 1$, $\tau_R = 0.9$.

chains are nonzero and equal. The quality factors exhibit a slightly greater robustness against variations of a single onsite energy [Fig. 7(a,b)], achieving values close to 20% for detuning values of $\epsilon_1/\Delta = 0.5$. When both QD energies of the outer chains equally large, the quality factors degrade faster than when a single QD has a nonzero energy; see Fig. 7(c,d).

While these QD energies seem to be detrimental, it is worth noting that they also bring additional functionality for the nonlocal Josephson diode. To see this, we first notice that the polarity of the diode, reflected in the sign of η_L , is highly controllable by the phase across the junction between the middle and right chains ϕ_R . The diode's polarity is also determined by strength of ETC and CAR, as observed in Fig. 7. Notably, the nonzero values of the onsite energies in the outer chains have the capability to change the diode's polarity around $\phi_R = \pi$. Depending on whether a single ϵ_1 or both $\epsilon_{1,2}$ energies are varied, the change in the diode's polarity can be fast or slow, respectively. Since the QD energies are expected to be tunable by means of gates [59], $\epsilon_{1,2}$ add important control of the nonlocal Josephson diode effect discussed here.